Supporting Information

A Single-Component Photorheological Fluid with Light-Responsive Viscosity

Elaine A. Kelly,[a] Niamh Willis-Fox,[b] Judith E. Houston,[c] Camille Blayo,[d] Giorgio Divitini,[a] Nathan Cowieson,[e] Ronan Daly[b] and Rachel C. Evans*[a]

[a] Department of Materials Science and Metallurgy, University of Cambridge, 27 Charles Babbage Rd, Cambridge CB3 0FS, UK

[b] Institute for Manufacturing, Department of Engineering, University of Cambridge. 17 Charles Babbage Rd, Cambridge CB3 0FS, UK

[c] European Spallation Source ERIC, Box 176, SE-221 00 Lund, Sweden

[d] School of Chemistry, Trinity College Dublin, College Green, Dublin 2, Ireland

[e] Diamond Light Source, Harwell Science and Innovation Campus, Didcot, Oxfordshire, OX11 0DE, United Kingdom

* Corresponding Author: rce26@cam.ac.uk

Table of Contents

1. Synthesis and Characterisation

Materials

Sodium nitrite ($NaNO_3$, ≥99.0%), anhydrous potassium carbonate (≥99.0%), potassium iodide (KI, 99.0%), sodium hydride (60% w/w in mineral oil), tetraethylene glycol (99%), hydrochloric acid (HCl, conc. 37%), ethanol (HPLC grade), tetrahydrofuran (THF, HPLC grade), dichloromethane, acetone and were purchased from Sigma Aldrich. 4-hexylaniline (90%) was purchased from ChemCruz. Sodium hydroxide (NaOH, ≥97%) and chloroform (>99%) were purchased from Fisher Scientific and phenol (>99.0%) was purchased from BDH Chemical Ltd. England. 1,4-dibromobutane (>98%) was purchased from Alfa Aesar. All reagents and solvents were used as received unless otherwise stated.

Methods

The synthesis of the $C_6AzoOC_4E_4$ was achieved through three steps: (1) the preparation of a hydroxyl precursor, 4-hexyl-4′-hydroxylazobenzene; (2) modification of the above to a bromoprecursor, 4-hexyl-4′-(2-bromo)butyloxy azobenzene, via an SN2 reaction; (3) addition of the neutral tetraethylene glycol head group to yield the final product, $C_6AzoOC_4E_4$.

(1) Synthesis of C6AzoOH (4-hexyl-4'-hydroxyl azobenzene)

In a 100 mL round-bottom flask, 4-hexylaniline (3.85 mL, 20 mmol) was dissolved in an acetone: water mixture (1:1, 50 mL) and HCl (37.5%, 0.048 mol, 4 mL) added. The resulting orange solution was placed in an ice bath and kept at 0 °C. Sodium nitrite (20 mmol, 1.38 g) was dissolved in distilled water (20 mL), cooled (1-2 °C) and added dropwise to the acidic alkylaniline solution. The orange solution was left to stir over ice for 5 min, to allow for diazonium salt formation. The solution was placed in the freezer until required. Separately, NaOH (20 mmol, 0.8 g), Na_2CO_3 (20 mmol, 2.12 g) and phenol (20 mmol, 1.88 g) were dissolved in distilled water (50 mL) and cooled until the solution temperature reached 1-3 °C. To this basic solution, the acidic diazonium salt solution was added dropwise, maintaining a temperature below 8 °C. An aqueous NaOH solution (6.5 mL, 2.5 mmol L^{-1}) was added dropwise to the basic phenol solution along with the acidic diazonium salt solution, in order to maintain a final pH of 10. The resulting yellow precipitate was filtered and washed with cold water. C_6AzoOH was recovered in the form of a yellow powder.

^{1}H NMR: ($CDCl_3$, 400 MHz, 25 °C): δ = 0.91 (t, J = 8 Hz, 3H), 1.34 (m, 6H), 1.68 (m, 2H), 2.67 (t, J = 9 Hz, 2H,), 5.06 (s, 1H.), 6.98 (d, J = 7 Hz, 2H), 7.33 (d, J = 8.4 Hz, 2H), 7.81 (d, J = 7.2 Hz, 2H), 7.88 (d, J = 8.4 Hz, 2H) ppm.

^{13}C NMR: ($CDCl_3$, 100 MHz, 25 °C): δ = 14.1, 22.6, 28.9, 31.3, 31.7, 35.9, 115.8, 122.5, 124.8, 129.1, 146, 147.2, 150.9, 158.2 ppm.

FTIR: v = 3547 (w), 3292 (b), 2956 (s), 2916 (s), 2849 (s), 1646 (w), 1586 (s), 1478 (C-H, s), 1404 (, s), 1290 (s), 1142 (s), 830 (s) cm^{-1}.

Mass Spectrometry (CH_3Cl, m/z: $APCI^+$): Exact mass calculated: 282.1732 [M], exact mass obtained: 281.1659 $[M-H]^+$.

Melting Point: 86.9 – 88.8 °C.

Yield: 74%

(2) Synthesis of bromoprecursor C6AzoOC$_4$Br (4-hexyl-4'(4-bromo)alkoxy azobenzene):

C_6AzoOH (1 eq., 10 mmol, 2.82 g), was dissolved in acetone (25 mL). 1,4 di-bromobutane (2 eq., 20mmol, 2.39 mL), K_2CO_3 (2 eq., 20 mmol, 2.76 g) and KI (0.1 eq., 1 mmol, 0.17 g) were added and the resulting dark red solution was stirred under reflux at 65 °C for 2 days with monitoring *via* thin layer chromatography (TLC, 9:1 cyclohexane: ethyl acetate). When the reaction reached completion, acetone was removed *via* rotary evaporation and the product dissolved in dichloromethane (DCM, 20 mL) and washed with water to remove the co-salt. DCM was removed *via* rotary evaporation and C_6AzoOC$_4$Br was recovered as an orange solid upon recrystallisation from ethanol.

^{1}H NMR: ($CDCl_3$, 400 MHz, 25 °C): δ = 0.92 (t, J = 8 Hz, 3H), 1.35 (m, 6H), 1.68 (m, 2H), 2.06 (m, 4H), 2.7 (t, J = 6.6 Hz, 2H), 3.47 (m, 2H), 4.11 (t, J = 6 Hz, 2H) 7.03 (d, J = 8.8 Hz, 2H), 7.29 (d, J = 8.2 Hz), 7.81 (d, J = 8.3 Hz 2H), 7.9 (d, J = 8.9 Hz, 2H) ppm.

^{13}C NMR: **($CDCl_3$, 400 MHz, 25 °C):** δ = 14.1, 22.6, 27.9, 29, 31, 31.3, 32.5, 33.4, 35.9, 67.2, 119.7, 122.6, 124.6, 129.1, 145.9, 147.1, 151, 161.1 ppm.

FTIR: v = 2914 (s), 2848 (w), 1602 (s), 1498 (s), 1380 (w), 1256 (s), 1133 (s) cm^{-1}.

Mass Spectrometry (CH_3Cl, m/z: APCI): Exact mass calculated: 416.1463 [M], exact mass obtained: 417.154 $[M+H]^+$

Melting Point: 136.2 - 137.5 °C

Yield: 85%

(3) Synthesis of C_6AzoOC$_4$E$_4$ (4-hexyl-4'-(mono-tetraethylene glycol) butyloxy azobenzene:

Tetraethylene glycol (5 eq., 28.1 mmol, 5.41 mL) was dried azeotropically by distillation with toluene (20 mL) at 170 °C. Dry tetraethylene glycol was then dissolved in dry THF (25 mL) in a round-bottomed flask (50 mL) under an inert N_2 atmosphere. To this NaH (60% in oil (w/w), 1.5 eq., 8.4 mmol, 0.346 g) was added and left to stir for 1 h under N_2. C_6AzoOC$_4$Br (1.0 eq., 2.3 g, 5.6 mmol) was dissolved in dry THF (10 mL) and added to the reaction flask. The resulting red solution was refluxed at 65 °C for 24 h. Acetone was removed *via* rotary evaporation and the resulting red oil dissolved in dichloromethane (20 mL) and washed with water. The DCM layer was dried, filtered and the solvent was removed *via* rotary evaporation. Excess bromoprecursor was removed using a silica plug and washing with chloroform. The product was recovered with acetone and the solvent removed to yield **C_6AzoOC$_4$E$_4$** as a red oil in 39% yield.

^{1}H NMR: ($CDCl_3$, 400 MHz, 25 °C): δ = 0.90 (t, J = 8 Hz, 3H), 1.22 (d, 2H), 1.33 (m, 6H), 1.66-1.9 (m, 6H), 2.69 (t, J = 8 Hz, 2H), 3.63 (m, 16H), 4.09 (t, J = 7 Hz, 2H), 7 (d, J = 8.88 Hz, 2H), 7.30 (d, J = 8.16 Hz, 2H), 7.80 (d, J = 8.2 Hz, 2H), 7.89 (d, J = 8.8 Hz, 2H) ppm.

^{13}C NMR: ($CDCl_3$, 600 MHz, 25 °C): δ = 14.1, 22.6, 26.1, 28.9, 30.9, 31.3, 31.7, 35.4, 61.7, 68, 70-70.9 (7 peaks), 72.6, 114.7, 122.5, 124.6, 129.0, 145.8, 146.9, 151.0, 161.4 ppm

FTIR: v = 3175 (br), 2959 (w), 2926 (m), 2873 (w), 1603 (s), 1490 (m), 1256 (s), 1131 (m) cm^{-1}

Mass Spectrometry (CH_3Cl, m/z: APCI$^+$): Exact mass calculated: 530.3356. Exact mass obtained: 531.3442 $[M+H]^+$.

2. Critical Micelle Concentrations

Table S1. The critical micelle concentrations (*cmc*s) of the *trans*- and *cis*- isomers have been reported elsewhere[1] and were determined using dynamic light scattering and surface tensiometry. The errors are given in brackets and were determined from the standard deviation of three measurements.

	***cmc* by ST** ($\times 10^{-6}$ M)		***cmc* by DLS** ($\times 10^{-6}$ M)	
	trans-isomer	*cis*-isomer	*trans*-isomer	*cis*-isomer
C_6AzoOC_4E$_4$	37.1 (6.3)	29.5 (1.8)	22.9 (4.2)	23.7 (5)

3. Determining the Composition of the Photostationary State

The degree of isomerisation in the *cis*-photostationary state (PSS) can be calculated from:[2]

$$ID_{trans-cis} = \frac{A(0)_{350} - A(PSS)_{350}}{A(0)_{350}} \times 100\% \qquad \text{Eq. S1}$$

where $A(0)_{350}$ refers to the absorbance of the assembly of 100% *trans*-isomers at 350 nm and $A(PSS)_{350}$ refers to the absorbance of the *cis*-PSS at 350 nm. Similarly, for reverse isomerisation, a majority *trans*-PSS is obtained by:

$$ID_{cis-trans} = \frac{A(PSS)_{350}}{A(0)_{350}} \times 100\% \qquad \text{Eq. S2}$$

$A(PSS)_{350}$ now refers to the absorbance of the *trans*-PSS at 365 nm.

4. Confirming the Presence of the *cis*-PSS for Post-Rheology Samples

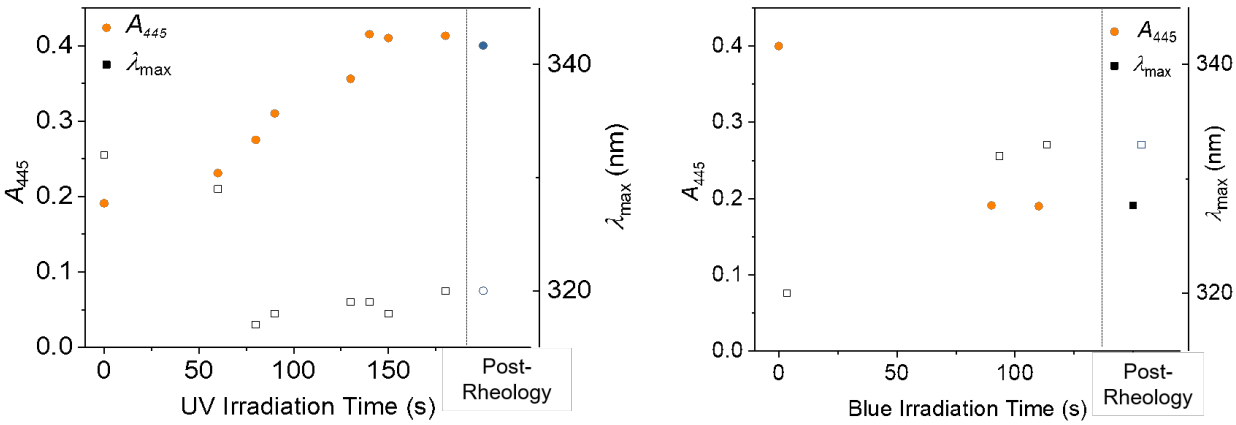

Figure S1. UV-Vis absorption spectra were collected on aliquots of C_6AzoOC_4E$_4$ (2.5 wt% parent solution, aliquots diluted for UV-Vis absorption measurements) removed during the light irradiation process (either UV or blue) and after rheology measurements. (a) Under UV irradiation, the presence of the *cis*-isomer is characterised by the increase in the absorbance of the n → π* band (445 nm) and a absorption maximum (λmax) of 318 nm. (b) The return to the *trans*-isomer dominant state under blue irradiation is characterised by a decrease in absorption at 445 nm and λmax of 332 nm.

5. Analysis of Rheological Behaviour

The Maxwell model used to fit the dynamic rheology measurements is given by Equations S3 and S4.

$$G'(\omega) = \frac{\omega^2 \tau_R^2 G_0}{1+\omega^2 \tau_R^2} \quad \text{(Eq. S3)}$$

$$G"(\omega) = \frac{\omega \tau_R G_0}{1+\omega^2 \tau_R^2} \quad \text{(Eq. S4)}$$

where ω is the frequency of the applied sinusoidal deformation, τ_R is the relaxation time of the WLM and G_o is the plateaus modulus. A crossover from G' < $G"$ to G' > $G"$ with increasing frequency is consistent with this viscoelastic, Maxwellian behaviour and is generally taken as a strong suggestion of wormlike micelles.[3,4]

An additional means to confirm the presence of a viscoelastic fluid with Maxwellian behaviour is *via* a Cole-Cole plot (Eq. S5). A plot of G' vs $G"$ should trace a semi-circle with a radius equal to the crossover frequency obtained from oscillatory measurements.[5–7]

$$G"^2 + (G' - \frac{G_0}{2})^2 = (\frac{G_0}{2})^2 \quad \text{(Eq. S5)}$$

The complex viscosity, $|\eta^*|$ is related to the zero-shear viscosity, η_0, by:

$$|\eta^*| = \frac{\sqrt{G'^2+G"^2}}{\omega} = \frac{\eta_0}{\sqrt{1+\omega^2\tau_R^2}} \quad \text{(Eq. S6)}$$

6. Oscillatory Rheology Measurements after Blue Light Irradiation

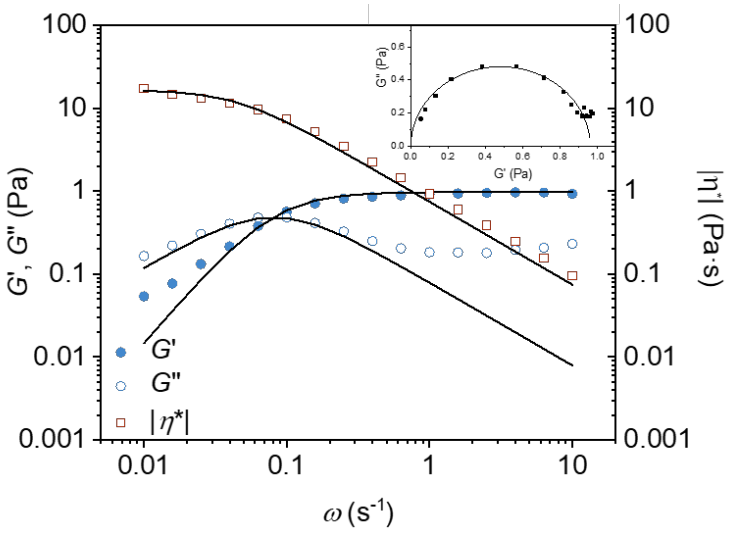

Figure S2. Variation of storage (G') and loss ($G"$) moduli and complex viscosity ($|\eta^*|$) with angular frequency (ω) for $C_6AzoOC_4E_4$ (2.5 wt% in H_2O) recovered from the *cis*-PSS with blue light illumination. Black lines are fits to a Maxwell model. Inset: A Cole-Cole plot traces a semi-circle with a radius equal to the crossover frequency (ω_c).

7. Calculation of the Packing Parameter

Table S2. Contributions of volumes, lengths and effective areas to calculate the packing parameter, *P*, using the additivity principle.

Component	Values	Method
Alkyl chain volume (nm^3)	0.0269m + 0.0274	Tanford equations[8]
Azobenzene volume (nm^3)	0.176/0.177 (*trans*/*cis*)	MOPAC calculations, van der Waals volume[9]
Oxy-group volume (nm^3)	9.1×10^{-3}	*Ab initio* calculations, van der Waals volume[10]
Alkyl chain length (nm)	0.1265m + 0.15	Tanford equation[8]
Azobenzene length (nm)	0.9/0.55 (*trans*/*cis*)	X-ray analysis[11]
Oxy-group length (nm)	0.28	DFT calculations[12]
E_4 effective area (nm^2)	0.46	ST study of $C_{12}E_4$ at 25 °C[13]

8. Model Fitting to Small-Angle X-ray Scattering Data

The cylinder model used here describes a right circular cylinder with uniform scattering length density. The output of the 1D scattering intensity function for randomly oriented cylinders is given by:[14,15]

$$P(q,\alpha) = \frac{1}{V}\int_0^{\frac{\pi}{2}} F^2(q,\alpha)\sin(\alpha)\,d\alpha \qquad \text{(Eq. S7)}$$

where α is the angle between the axis of the cylinder and the vector *q* and *V* is the volume of the cylinder. *F* is given by:

$$F(q,\alpha) = 2(\Delta\rho)V\frac{sin\left(qLcos\left(\frac{\alpha}{2}\right)\right)}{qLcos\left(\frac{\alpha}{2}\right)}\frac{J_1(qrsin(\alpha))}{qrsin(\alpha)} \qquad \text{(Eq. S8)}$$

where $\Delta\rho$ is the contrast (scattering-length density difference between the scattering body and solvent), *L* is the length of the cylinder, *r* is the radius of the cylinder and J_1 is the first order Bessel function.

For the flexible cylinder model, the cylinder is considered as a chain of contour length, L_C, comprised of a number of locally stiff segments, the length of which is given by the persistence length, l_p. The Kuhn length, L_K is the length over which the flexible cylinder can be considered as a rigid rod and is given by $L_k = 2l_p$. The cross-sectional radius of the cylinder segment is

given by R_{CS}. The non-negligible diameter of the cylinder is included in this model by accounting for excluded volume interactions within the walk of a single cylinder. Inter-cylinder interactions are not accounted for. Overall, the scattering function, (S(*q*, *L* ,*b*)), of a semi-flexible chain with a uniform scattering length density, taking excluded volume effects into account is given by:[17,18]

$$S(q,L,b) = [1 - w(qR_g)S_{Debye}(q,L,b) + f_{corr}(q)w(qR_g)[1.22(qR_g)^{\frac{-1}{0.585}} + 0.4288(qR_g)^{-\frac{2}{0.585}} - 1.651(qR_g)^{\frac{-3}{0.585}}] + \frac{Cn_b}{n_b}\{\frac{4}{15} + \frac{7}{15u} - \left(\frac{11}{15} + \frac{7}{15u}\right) \times e^{-u(q,L,b)}\} \quad \text{(Eq. S12)}$$

where w(*qRg*) is an empirical crossover function, n_b = *L*/*b* and $f_{corr}(q)$ is a correction factor added by Chen *et al*. to correct unphysical errors occurring at certain *L*/*b* ratios.[18] Further details of $f_{corr}(q)$, w(*qRg*), $S_{Debye}(q, L, b)$and *u*(*q, L, b*) can be found in the work of Pederson *et al.*[17] and Chen *et al.*[18] This form factor is normalised by particle volume, averaging over all possible orientations of the flexible cylinder.

Any polydispersity in the cylinder radius (cylinder model, flexible cylinder model) or Kuhn length (flexible cylinder model) was accounted for using a lognormal description for the polydispersity, where for a function of *x*, ln(*x*) has a normal distribution, defined as:

$$f(x) = \frac{1}{Norm}\frac{1}{x\sigma}exp(-\frac{1}{2}(\frac{ln(x)-\mu}{\sigma})^2) \quad \text{(Eq. S13)}$$

where *Norm* is the normalisation factor, determined during the numerical calculation, $\mu = \ln(x_{med})$, x_{med} is the median value of the lognormal distribution and σ describes the width of the underlying normal distribution. The polydispersity in the cylinder and flexible cylinders as used here is given by:

$$PD = \sigma = \frac{p}{x_{med}} \quad \text{(Eq. S14)}$$

The mean value of the distribution is given by $x = \exp\left(\frac{\mu+\sigma^2}{2}\right)$ and the peak value by $\max x = \exp(\mu - \sigma^2)$.

Table S3: Structural parameters obtained from SAXS data for *trans*- and *cis*-$C_6AzoOC_4E_4$ in H_2O (0.5 and 2.5 wt%) at 25 °C. *R* is cylinder radius obtained from the best fit to the data using the model specified in column 3. L_K is the Kuhn length obtained from the best fit to the data using the flexible cylinder model, *L* is the value for cylinder or contour length obtained from fitting to the model specified in column 3, PD_r is the polydispersity applied to the cylinder radius, PD_{Lk} is the polydispersity applied to the Kuhn length. The scattering length density (SLD) of the sample was calculated to be 9.62 x 10^{-6} $Å^{-2}$, while that of the solvent is 9.44 x 10^{-6} $Å^{-2}$. All model fittings were performed in SasView.

Isomer	wt%	Model	*R* (Å)	L_K (Å)	*L* (Å)	PD_r	PD_{Lk}	χ^2
trans	0.5	Cylinder	46.9	-	*	0.27		1.74
trans	2.5	Flexible Cylinder	58.9	618.2	*	0.27	0.15	4.79
cis	0.5	Flexible Cylinder	42.1	100.8	*	0.28	-	0.60
cis	2.5	Flexible Cylinder	42.0	177.2	*	-	-	1.00

*all cylinder lengths were fixed outside the observation window

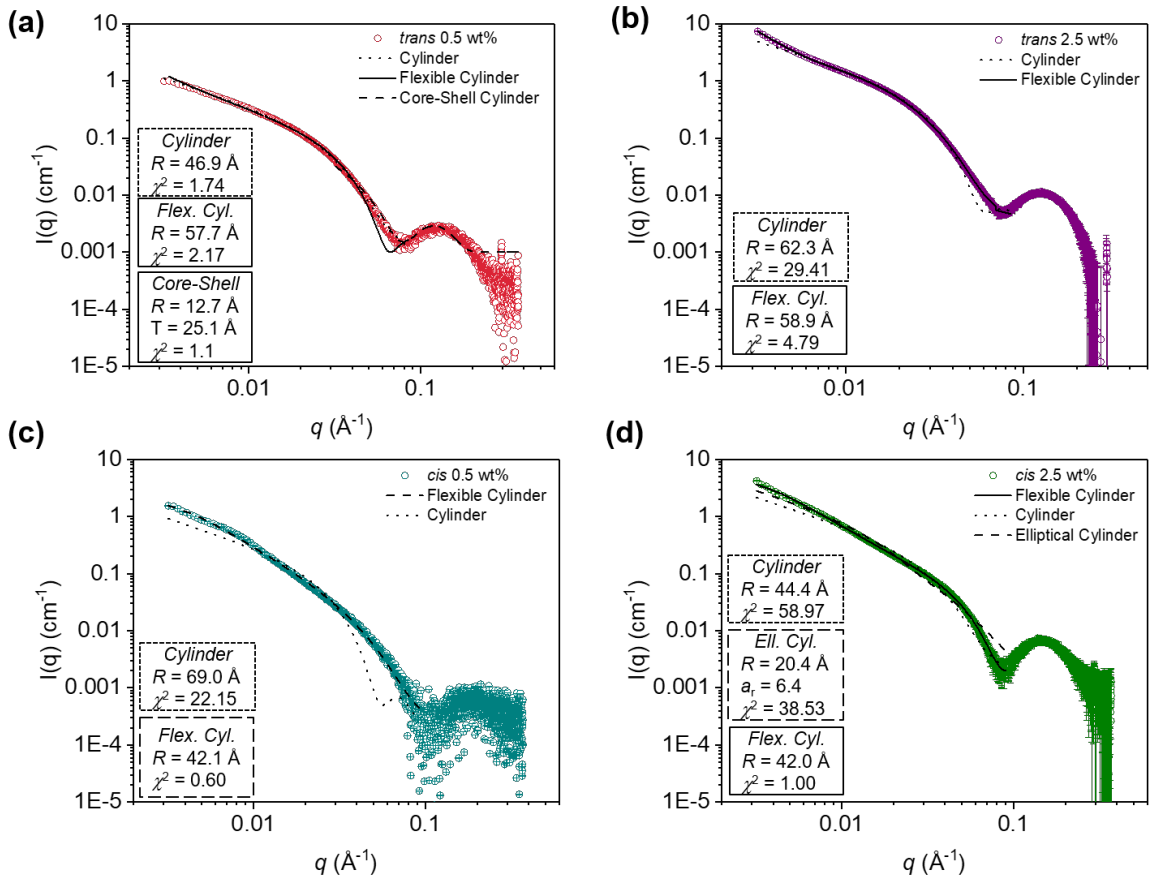

Figure S3. SAXS profiles of $C_6AzoOC_4E_4$ (a) *trans* 0.5 wt% (b) *trans* 2.5 wt% (c) *cis* 0.5 wt%, (d) *cis* 2.5 wt%, green) with different cylindrical models. Fits to the data are indicated by a dotted line (cylinder model), a dashed line (elliptical cylinder model) and a solid line (flexible cylinder model). The core-shell model is only fitted to high *q* for *trans* 0.5 wt%. The cylinder radius (*R*), and goodness-of-fit (χ^2) are given to facilitate comparison between the models.

9. Additional Cryo-TEM Images

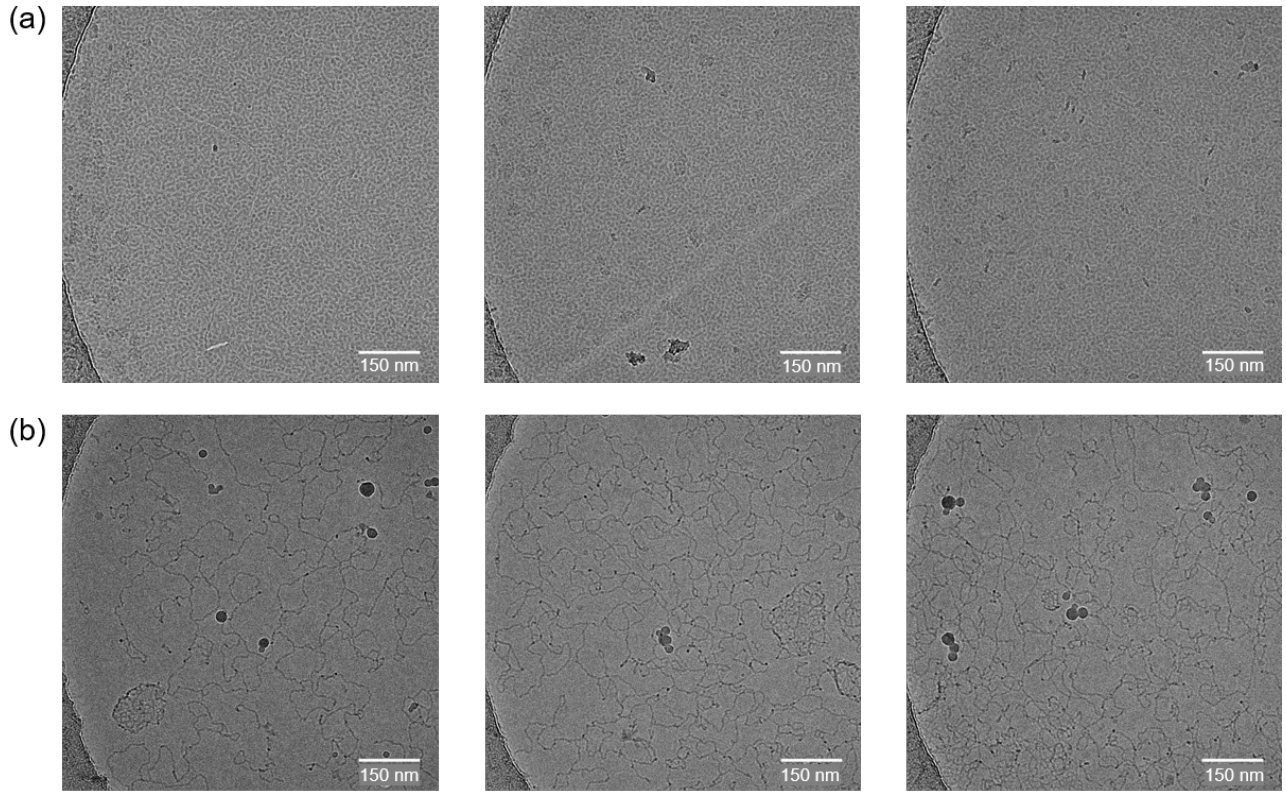

Figure S4. Cryo-TEM images of $C_6AzoOC_4E_4$ (2.5 wt%, H_2O) before (a) and after (b) 90 mins UV illumination. Scale bar indicates 150 nm.

10. References

[1] J. E. Houston, E. A. Kelly, M. Kruteva, K. Chrissopoulou, N. Cowieson and R. C. Evans, *J. Mater. Chem. C*, **2019**, 7, 10945–10952.

[2] S. Peng, Q. Guo, P. G. Hartley and T. C. Hughes, *J. Mater. Chem. C*, **2014**, 2, 8303–8312.

[3] M. E. Cates, *Macromolecules*, **1987**, 20, 2289–2296.

[4] M. E. Cates and S. J. Candau, *J. Phys. Condens. Matter*, **1990**, 2, 6869–6892.

[5] J. Yang, Z. Yang, Y. Lu, J. Chen and W. Qin, *J. Dispers. Sci. Technol.*, **2013**, 34, 1124–1129.

[6] B. Song, Y. Hu, Y. Song and J. Zhao, *J. Colloid Interface Sci.*, **2010**, 341, 94–100.

[7] D. Xie, D. You, S. Ying, B. Song and J. Tian, *RSC Adv.*, **2017**, 7, 48120–48126.

[8] C. Tanford, *J. Phys. Chem.*, **1972**, 76, 3020–3024.

[9] K. Takeshita, N. Hirota and M. Terazima, *J. Photochem. Photobiol. A Chem.*, **2000**, 134, 103–109.

[10] H. Durchschlag and P. Zipper, *Progr. Colloid. Polym. Sci*, **1994**, 94, 20–39.

[11] E. Merino and M. Ribagorda, *Beilstein J. Org. Chem.*, **2012**, 8, 1071–1090.

[12] F. Agapito, B. J. Costa Cabral and J. A. Martinho Simões, *J. Mol. Struct. THEOCHEM*, **2005**,

729, 223–227.

[13] M. J. Rosen and M. Dahanayake, *J. Phys. Chem.*, **1982**, 25, 541–545.

[14] J. S. Pederson, *Adv. Colloid Interface Sci.*, **1997**, 70, 171–210.

[15] A. Guiner and G. Fournet, *Small Angle Scattering of X-rays*, Wiley, 1955.

[16] L. . Feigin and D. . Svergun, *Structure Analysis by Small Angle X-ray and Neutron Scattering*, Plenum, New York, 1987.

[17] J. S. Pedersen and P. Schurtenberger, *Macromolecules*, **1996**, 29, 7602–7612.

[18] W. R. Chen, P. D. Butler and L. J. Magid, *Langmuir*, **2006**, 22, 6539–6548.